MOLECULAR ECOLOGY

Widespread intersex differentiation across the stickleback genome – the signature of sexually antagonistic selection?

Journal:	*Molecular Ecology*
Manuscript ID	MEC-19-0741.R1
Manuscript Type:	Original Article
Date Submitted by the Author:	n/a
Complete List of Authors:	Bissegger, Mirjam; University of Basel, Department of Environmental Sciences Laurentino, Telma; University of Basel, Department of Environmental Sciences Roesti, Marius; University of Bern, Institute of Ecology and Evolution Berner, Daniel; University of Basel, Zoological Institute
Keywords:	Fish, Genomics/Proteomics, Population Genetics - Empirical, Sexual Selection

Widespread intersex differentiation across the stickleback genome – the signature of sexually antagonistic selection?

Mirjam BISSEGGER[1], Telma G. LAURENTINO[1], Marius ROESTI[2], Daniel BERNER[1*]

[1] Department of Environmental Sciences, Zoology, University of Basel, 4051 Basel, Switzerland

[2] Institute of Ecology and Evolution, University of Bern, 3012 Bern, Switzerland

[*] correspondence: daniel.berner@unibas.ch, +41 (0)61 207 0328

Abstract

Females and males within a species commonly have distinct reproductive roles, and the associated traits may be under perpetual divergent natural selection between the sexes if their sex-specific control has not yet evolved. We here explore whether such sexually antagonistic selection can be detected based on the magnitude of differentiation between the sexes across genome-wide genetic polymorphisms by whole-genome sequencing of large pools of female and male threespine stickleback fish. We find numerous autosomal genome regions exhibiting intersex allele frequency differences beyond the range plausible under pure sampling stochasticity. Alternative sequence alignment strategies rule out that these high-differentiation regions represent sex chromosome segments misassembled into the autosomes. Instead, comparing allele frequencies and sequence read depth between the sexes reveals that regions of high intersex differentiation arise because autosomal chromosome segments got copied into the male-specific sex chromosome (Y), where they acquired new mutations. Because the Y chromosome is missing in the stickleback reference genome, sequence reads from derived DNA copies on the Y chromosome still align to the original homologous regions on the autosomes. We argue that this phenomenon hampers the identification of sexually antagonistic selection within a genome, and can lead to spurious conclusions from population genomic analyses when the underlying samples differ in sex ratios. Because the hemizygous sex chromosome sequence (Y or W) is not represented in most reference genomes, these problems may apply broadly.

Keywords

Allele frequency / Duplication / *Gasterosteus aculeatus* / Genome assembly / Population genomics / Repetitive DNA / Sex chromosome

INTRODUCTION

In organisms with distinct sexes, different female and male reproductive strategies may imply that selective trait optima differ between the sexes (Arnqvist & Rowe, 2005; Darwin, 1871; Slatkin, 1984; Shine, 1989). Because the sexes share most of their genome and alleles typically have similar effects in both sexes (Poissant, Wilson, & Coltman, 2010), this can result in a conflict in that alleles improving a trait in one sex may push the same trait away from its optimum in the other sex (Arnqvist & Rowe, 2005; Rice & Chippindale, 2001). Such sexually antagonistic selection (hereafter 'SAS') may weaken with the emergence of stable sex-specific gene expression and the associated sexual dimorphism. The resolution of sexual antagonism will typically involve the establishment of a link between a preexisting molecular signal derived from the sex-determination pathway, and a newly gained binding site for that sex-specific signal controlling the level of expression of the selected gene (Stewart, Pischedda, & Rice, 2010; Williams & Carroll, 2009). This resolution process, requiring at least one highly specific mutation, is suggested to be slow (Stewart et al., 2010) and often appears incomplete in natural populations (Cox & Calsbeek, 2009). Moreover, the presence and strength of SAS may plausibly vary over time and between ecologically different environments. For these reasons, genetic polymorphisms under SAS may well be widespread across the genomes of natural populations and may make a substantial contribution to maintaining genetic variation within these populations (Connallon & Clark, 2014; Cox & Calsbeek, 2009; Rice & Chippindale, 2001).

Recent genomic investigations, performed mainly in genetic model organisms, indeed seem to support the notion that loci under SAS are common within the genome (Cheng & Kirkpatrick, 2016; Dutoit et al., 2018; Griffin, Dean, Grace, Ryden, & Friberg, 2013; Innocenti & Morrow, 2010; Lucotte, Laurent, Heyer, Ségurel, & Toupance, 2016). These investigations typically infer genes putatively under SAS based on the skew in the magnitude of gene expression between the sexes, as estimated by transcriptomic analysis. Challenges with this approach include ambiguity in the extent to which sex-biased gene expression indicates current intersexual conflict, and methodological difficulties in estimating sex-bias in gene expression reliably (Mank, 2017; Stewart et al., 2010). In principle, a conceptually simple approach to exploring SAS across a genome without using gene expression data exists: if sexual antagonism occurs throughout ontogeny and thus causes divergent viability selection between the sexes (Cox & Calsbeek, 2009; Rice & Chippindale, 2001; Shine, 1989; Slatkin, 1984), the underlying loci should display frequency differentiation between the sexes in the adult stage, with female-beneficial alleles enriched in females and male-beneficial alleles enriched in males. In the beginning of every new generation, however, this intersex differentiation should be erased due

to the random assortment of female- and male-beneficial alleles during reproduction. Whether allele frequency differentiation due to divergent viability selection between females and males can be detected in genome-wide screens should depend on the number of antagonistically selected loci, and on the strength of selection on these – thus representing an empirical issue. An analysis in humans suggests that a genome-wide signature of SAS can be detected based on female-male differentiation data alone (Lucotte et al., 2016), but evidence from further organisms is needed.

We here investigate potential signatures of SAS based on genome-wide intersex differentiation data in threespine stickleback fish (*Gasterosteus aculeatus*). The motivation for this study is twofold. First, in threespine stickleback, males and females play distinct reproductive roles (Östlund-Nilsson, Mayer, & Huntingford, 2007): during the reproductive period, females allocate resources primarily into egg production, whereas males hold territories and perform brood care. The sexes also appear to exploit distinct ecological niches, as indicated by sexual dimorphism in parasite communities (Reimchen & Nosil, 2001), in predator defense traits (Reimchen & Nosil, 2004), and in trophic morphology (Aguirre & Akinpelu, 2010; Berner, Roesti, Hendry, & Salzburger, 2010; Bolnick & Lau, 2008; Kitano, Mori, & Peichel, 2007; Kristjansson, Skulason, & Noakes, 2002; Spoljaric & Reimchen, 2008). Sexual dimorphism in trophic morphology is particularly pronounced in habitats in which disruptive selection due to intraspecific resource competition is inferred to be strongest (Bolnick & Lau, 2008). Divergence between the sexes in trophic traits cannot plausibly be ascribed to sexual selection and must therefore reflect differential trait optimization by natural selection within each sex (Darwin, 1871; Selander, 1966; Shine, 1989; Slatkin, 1984; Rice & Chippindale, 2001). The opportunity for sexual antagonism mediated by divergent viability selection during ontogeny thus seems given in this species.

The second impetus to our study is the observation of a few autosomal single-nucleotide polymorphisms (SNPs) showing substantial differentiation between females and males in a preliminary genomic screen (M. Roesti & D. Berner, unpublished data; an example is shown in Figure S1 in the Supplemental Information). This analysis, however, used sequence data with reduced genomic representation (RAD sequencing) (Roesti, Kueng, Moser, & Berner, 2015) and was based on a low number of individuals from each sex (12 females, 13 males), thus making pattern interpretation difficult. We here overcome these methodological limitations by a formal analysis of intersex genetic differentiation across the full stickleback genome based on large sample sizes. As we will show, regions exhibiting strong intersex genetic differentiation are abundant across the stickleback autosomal genome. Scrutinizing the cause for intersex

differentiation in these regions, however, highlights a general methodological challenge to evolutionary genomic analysis, rather than providing evidence of SAS.

MATERIALS AND METHODS

Study design, sampling and DNA extraction

Our approach to investigating genomic regions potentially showing signatures of SAS in stickleback was to generate a female and a male pool of DNA, each representing a large number of individuals, to perform whole-genome sequencing of these pools, and to subject the resulting polymorphism data to a genome-wide screen for the magnitude of intersex differentiation.

We used stickleback individuals sampled from Lake Constance (Switzerland) at the ROM study site (Berner et al., 2010; Moser, Roesti, & Berner, 2012) from April to June 2016 for a behavioral experiment (Berner et al., 2017). Sample size for each sex-specific DNA pool was 120 individuals (i.e., 240 haploid genomes per sex). To standardize the contribution of individual DNA to the final pool, we pierced a disk of 2 mm diameter form the spread caudal fin of each individual by using a biopsy puncher (KAI Medical, Gifu, Japan). Within each sex, these individual tissue samples were combined into 12 sub-pools of 10 individuals per sex, and the sub-pools subjected to DNA extraction with the Qiagen DNeasy Blood & Tissue kit (Qiagen, Valencia, USA), including an RNAse treatment.

DNA pool preparation, sequencing and SNP discovery

After DNA quantitation of the 24 total sub-pools with a Qubit fluorometer (Thermo Fisher Scientific, Massachusetts, USA), they were combined without PCR enrichment at equimolar amounts to a single pool per sex. These pools were barcoded and whole-genome paired-end sequenced to 151 bases in two lanes of an Illumina HiSeq2500 instrument, each lane containing female and male DNA in similar parts. The raw sequence reads were demultiplexed by sex, pooled across the two sequencing lanes, and aligned to the third-generation assembly of the 447 Mb threespine stickleback reference genome (Glazer, Killingbeck, Mitros, Rokhsar, & Miller, 2015; hereafter 'reference genome') by using Novoalign v3.00 (http://www.novocraft.com/products/novoalign; seetings: -t540, -g40, -x12). The Rsamtools R package (Morgan, Pages, Obenchain, & Hayden, 2018) was then used to convert the alignments to BAM files, and to perform nucleotide counts at each base position using the *pileup* function (raw genome-wide nucleotide counts for each sex are provided on the Dryad repository). Median read depth across all genome-wide autosomal positions was 125 for females

and 137 for males. Combined with the large number of individuals used for sequencing pool preparation within each sex, this high read depth was expected to allow estimating allele frequencies highly accurately (Ferretti, Ramos-Onsins, & Perez-Enciso, 2013; Gautier et al., 2013). Next, the nucleotide counts of both sexes were pooled to determine if a given position was variable. SNPs were accepted if they displayed a read depth greater than 100 and lower than 800 across the female-male pool (median: 262), and if the minor allele frequency (MAF) in the pool was at least 0.15. The latter filter effectively removed sequencing errors and excluded SNPs having low sensitivity to capture selective shifts (Roesti, Salzburger, & Berner, 2012). A total of 1.63 million autosomal SNPs passed our read depth and MAF filtering, yielding an expected average marker density of one SNP per 255 bp.

Quantifying intersex differentiation through genome scans and simulations

We started our analysis of genomic differentiation between females and males by quantifying and visualizing the magnitude of intersex differentiation, expressed by the absolute allele frequency difference (AFD; Berner, 2019), across all chromosomes (the sex chromosome was included for completeness, although our focus lies on the autosomal genome). This genome scan revealed numerous genomic regions showing strong intersex differentiation (see Results & Discussion). Therefore, we next used simulations to compare the magnitude of intersex differentiation observed in the genome-wide scan to levels of differentiation expected under pure sampling stochasticity. We here thus aimed to develop a sense for the differentiation plausible in the absence of any deterministic factor driving sex bias in allele frequencies, such as SAS. We sampled alleles at random with replacement from a female and from a male pool at a SNP with two alleles occurring at the same frequency of 0.5 in both sexes. This assumption of the highest possible MAF led to conservative results because it maximized the sampling variance in allele frequencies, thus allowing for maximal intersex differentiation (see Figure 4 in Berner, 2019). The two samples were then used to calculate intersex AFD. Two sample sizes were considered: 50 per sex, approximating the minimum read depth required during SNP calling, and 120 per sex, approximating the median read depth observed (see above). In concordance with our empirical differentiation scan, the simulation included 1.63 million AFD estimates for each sample size.

Assessing the role of genome misassembly as cause for high intersex differentiation

Before considering that the genomic regions of high intersex differentiation observed in the above genome scan represented genuine signatures of SAS, it was essential to rule out methodological explanations. In a first step, we performed two analyses based on re-alignment

of our sequence reads. Specifically, threespine stickleback display divergent sex chromosomes (Peichel et al., 2004; Roesti, Moser, & Berner, 2013), with the females representing the homogametic (XX) and males the heterogametic (XY) sex. Strong intersex differentiation may thus simply emerge because homologous X and Y chromosome segments harboring single-nucleotide differences erroneously align to autosomal regions. This may occur due to either genome sequence divergence between our focal population (derived from an Atlantic marine ancestor) and the reference genome (representing an individual derived from a Pacific ancestor; Jones et al., 2012), or the incorrect placement of sex chromosome segments on autosomes in the reference genome assembly. To explore these possibilities, we assessed whether regions of strong differentiation still persisted when performing more stringent alignment (i.e., tolerating much lower sequence mismatch: -t200), which should reduce the likelihood of sex chromosome segments to erroneously align to autosomes. The sequence alignments resulting from this alternative alignment approach were used for a genome-wide scan for the magnitude of intersex differentiation as described above.

In addition, we aligned our raw sequence reads to a new threespine stickleback genome sequenced and assembled *de novo* (Berner et al., 2019), using the initial alignment settings. This new genome was derived from an individual sampled from the same watershed as our study population, thus ensuring minimal sequence divergence. The resulting sequence alignments were again used for a genome scan for intersex differentiation, which also indicated numerous regions of high differentiation. To assess whether these regions in the *de novo* genome corresponded to high-differentiation regions in our original scan, we chose a 151 bp sequence overlapping a high-differentiation SNP from a dozen of strongly differentiated regions located on different *de novo* genome scaffolds. We then evaluated visually the magnitude of differentiation in the 50 kb neighborhood around the alignment position of these sequences within the reference genome.

Testing if high intersex differentiation is driven by the lack of the Y chromosome sequence in the reference genome

After examining the possibility that autosomal regions of high differentiation emerged because of erroneous alignment of X and Y chromosome segments to autosomes, we evaluated a second methodological explanation. We here considered that both the reference genome and the new *de novo* genome are derived from a female (XX) individual. The Y chromosome is therefore necessarily missing in these genome assemblies. DNA segments closely related between autosomes and the Y chromosome may thus cause the alignment of Y-specific alleles to autosomes, thus potentially producing SNPs showing high intersex differentiation. This scenario

leads to two testable predictions (see also Dou et al., 2012; McKinney, Waples, Seeb, & Seeb, 2017; Tsai, Evans, Noorai, Starr-Moss, & Clark, 2019): first, the SNPs defining regions of high differentiation on autosomes should display a systematically higher MAF in the male than female pool because only males harbor the Y-specific allele that makes the given genome position polymorphic. Second, these SNPs should represent exclusively autosomal DNA in the females but autosomal *plus* Y chromosome segments in the males, and hence exhibit higher read depth in the male than female pool.

To test these two predictions, we first delimited a focal set of autosomal regions exhibiting high intersex differentiation (hereafter 'HIDRs' for High Intersex Differentiation Regions). Based on the distribution of intersex differentiation values observed empirically on the one hand, and the simulated distribution of differentiation under pure sampling stochasticity on the other hand (see below), HIDRs were required to harbor at least five SNPs showing AFD of 0.5 or greater within a window of 5 kilobases (kb). HIDRs further needed to be spaced by at least 100 kb from any other such region, to ensure independence. Given these criteria, we identified a total of 38 autosomal HIDRs. For each HIDR, we next selected at random a single representative high-differentiation SNP (AFD >= 0.5) exhibiting a sex-specific read depth of at least 50-fold, hereafter called 'HIDR SNP'. To obtain negative controls for statistical analysis, we also selected a 'control SNP' for each HIDR, defined as the SNP closest to the genomic position located 30 kb upstream of the corresponding HIDR SNP and passing the same read depth thresholds. For both SNP classes (i.e., HIDR and control), we then explored if there was sex-related skew in the MAF, and in read depth (quantified as read depth ratio, i.e., the nucleotide count of the male pool divided by the count of the female pool). The MAF data were analyzed visually based on histograms, while for the read depth ratio, we calculated median values for each SNP class along with their 95% bootstrap confidence intervals generated by 10,000 resamples (Manly, 2006).

Simulations exploring intersex differentiation in relation to selection strength

The above empirical analyses indicated that our detected HIDRs represented methodological artifacts (see Results & Discussion). To complement this evidence by theory, we additionally performed stochastic individual-based simulations exploring the magnitude of intersex differentiation resulting from SAS of different strengths on a single locus. The objective of this simulation analysis was not a comprehensive theoretical treatment, but to gain qualitative insight into the (im)plausibility of our HIDRs to reflect signatures of SAS.

We implemented a model starting with a population of 100,000 diploid individuals showing a balanced sex ratio. The locus under selection was bi-allelic with one allele favorable

in females and the other allele favorable in males (we thus assumed perfectly symmetric divergent selection, recognizing that in reality, the strength of selection on a polymorphism may differ between the sexes). The starting frequency of both alleles was 0.5. We modeled viability selection – as required if SAS should drive intersex differentiation within a generation – by making access to mating dependent on the genotype at the locus under selection (Berner & Roesti, 2017; Berner & Thibert-Plante, 2015). Specifically, an individual's probability of surviving to the reproductive stage was a stochastic function of the individual's deviation from the sex-specific optimum genotype. This deviation was determined by the number of unfavorable alleles times the selection coefficient, resulting in additive fitness. The genotypes of the females and males surviving to the reproductive stage were used to quantify the magnitude of intersex AFD observed after SAS within the focal generation. These individuals then mated at random, each pair producing a constant number of offspring (N = 10; using 4 or 20 offspring produced similar results; details not presented) that overall exactly re-established initial population size. Offspring sex was assigned at random. We considered selection coefficients of 0.01, 0.05, 0.1, 0.2, 0.3, 0.4, and 0.5, the latter representing the complete unviability (zero fitness) of individuals homozygous for the unfavorable allele. For each selection coefficient, we carried out ten replicate simulations, each running for 20 generations. We thus obtained a total of 200 estimates of within-generation intersex differentiation for a given selection strength. The simulation code is available on Dryad. Unless specified otherwise, all analyses were performed with the R language (R Development Core Team, 2018).

RESULTS AND DISCUSSION

Regions of strong intersex differentiation are widespread across stickleback autosomes

Allele frequency differentiation (AFD) between stickleback females and males showed a median magnitude of 0.053 across all genome-wide autosomal SNPs – but the distribution tapered off to a long tail reaching values up to 0.87 (Figure 1a). The latter strong intersex differentiation cannot be explained by pure sampling stochasticity, as revealed by comparing the empirical distribution of differentiation values to simulated distributions: even when modeling minimal sample size (N = 50) for each sex, and hence low precision in allele frequency estimation, differentiation values above 0.5 did not emerge across the 1.63 million replications (Figure S2). Assuming sample sizes more typical of our data set's read depth (N = 120), the top differentiation value observed in the simulations dropped to 0.32. Given that the simulations assumed the highest MAF possible (0.5; i.e., both alleles occurring in perfectly balanced proportions), even the latter upper simulation limit for differentiation due to sampling variation alone must be considered cautiously

high. Nevertheless, we used an AFD threshold of 0.5 for the identification of high-differentiation regions (HIDRs) in the analyses below.

Exploring the physical distribution of intersex differentiation values along chromosomes revealed narrow regions (typically a few kb wide) of high differentiation standing out clearly against background differentiation on all autosomes (Figure 1b; Figure 2a shows a representative example in high physical resolution, re-analyzed using F_{ST} as differentiation metric in Figure S3a; the complete differentiation plots for all chromosomes are presented as Figure S4).

Reference genome misassembly is not the cause for high intersex differentiation on autosomes

A chromosome exhibiting particularly extensive intersex differentiation along almost its entire length was the sex chromosome (chromosome XIX, Figure S4). Along this chromosome, differentiation primarily reflects the evolutionary divergence between the non-recombining regions of the X and Y sequences, with an additional contribution from reduced precision in allele frequency estimation in the hemizygous males (i.e., in males, the X chromosome occurs in a single copy only, thus causing systematically lighter read depth in the male pool). This observation motivated investigating whether regions of high intersex differentiation may be explained by the incorrect placement of DNA segments homologous but polymorphic between the X and Y chromosome into autosomes during reference genome assembly. Inconsistent with this idea, a genome scan for intersex differentiation based on sequence reads aligned to the reference genome with more stringent alignment settings did not produce results differing qualitatively from our initial genome scan: although read alignment success dropped from 81 to 69 percent with more stringent alignment, genomic regions showing high intersex differentiation in the initial genome scan were generally still present (details not presented). Similarly, aligning our sequence reads to a *de novo* stickleback genome assembly derived from an individual originating from the same watershed as our study population still revealed numerous genomic regions of high intersex differentiation. These regions consistently coincided with autosomal regions of high differentiation in our initial genome scan based on the reference genome (three examples are shown in Figure S5). Together, these two analyses using alternative alignment strategies make clear that the incorrect placing of sex chromosome segments within autosomes in the stickleback reference genome assembly fails as a general explanation for autosomal regions of high intersex differentiation.

High intersex autosomal differentiation arises from DNA segments shared between autosomes and the Y chromosome

Having ruled out reference genome misassembly as an explanation for strong autosomal differentiation between the sexes, we addressed a second hypothesis focused on reference genome *incompleteness*: that DNA segments similar to autosomal chromosome regions occur on the Y chromosome that is not part of any current genome assembly, and that these segments harbor private genetic variants that cause intersex differentiation when aligning to their autosomal counterparts (see also Tsai et al., 2019). Consistent with this idea, we observed that SNPs located within HIDRs showed a systematically reduced MAF in the female relative to the male pool (Figure 2b). More specifically, the majority of HIDR SNPs showed a female MAF of zero (i.e., monomorphism for one allele), while the male frequency was near 0.5 (i.e., the two SNP alleles occurred at relatively balanced frequency) (Figure 3 top). By contrast, the control SNPs showed a relatively uniform distribution of MAFs in both sexes (Figure 3 bottom). These observations make clear that the polymorphisms driving HIDRs arise from derived alleles restricted to the males.

The most plausible explanation for such male-specific alleles is that the DNA segments harboring these alleles are located on the Y chromosome. A unique prediction derived from this scenario is that the chromosome segments around HIDR SNPs should display elevated read depth in the male relative to the female sex. The reason is that only in males, these segments should recruit truly autosomal *plus* Y-chromosomal sequence reads aligning to the same location in the genome assembly. This prediction was confirmed unambiguously: the SNPs driving HIDRs very consistently exhibited elevated read depth in males compared to females (Figures 2c, 4). Such bias was absent in the control SNPs. (Note that the slight imbalance between the sexes at the control SNPs in Figure 4 is expected because the male DNA pool was sequenced to approximately 10% higher read depth; see Materials and Methods.) Interestingly, for the HIDR SNPs, the male-female read depth ratio showed a median of 2.18 (control SNPs: 1.06), with several SNPs displaying values beyond 3. If an autosomal segment was present as a single copy on the Y chromosome, however, one would expect a read depth ratio of 1.5. This leads us to propose a general model in which an autosomal DNA segment is first copied to the Y chromosome (see also Koerich, Wang, Clark, & Carvalho, 2008; Tsai et al., 2019), experiences mutation at the new location, and then – to variable extent – experiences further copy number expansion on the Y chromosome (Figure 5). Consistent with this model, the male-female read depth ratios of the HIDR SNPs tended to form distinct clusters overlapping with 1.5, 2, and 2.5 (Figure 4), as expected for autosomal segments falling into discrete copy number classes on the Y chromosome. Although the Y chromosome sequence of threespine stickleback is not yet available, our conceptual model is supported by the indication of an exceptionally high proportion of repeated DNA on a preliminary Y chromosome assembly as compared to all

autosomes (M. White & C. Peichel, personal communication; see also Chalopin, Volff, Galiana, Anderson, & Schartl, 2015; Hobza et al., 2017). As a definitive validation of our model, it would be worthwhile to determine the number of alignment sites of DNA segments representative of our HIDRs in a future Y chromosome assembly.

Simulations confirm the implausibility of sexually antagonistic selection as a cause for high autosomal intersex differentiation

Our empirical analyses clearly identified a methodological, non-selective explanation for regions of strong differentiation between the sexes across the stickleback genome. To nevertheless develop a sense for the magnitude of intersex differentiation in allele frequencies that viability selection could drive within a single generation, we used simulations of SAS on a single locus. We found that under the strongest selection considered – a heterozygous selection coefficient of 0.5, the sexes reach an allele frequency differentiation of 0.4 within each generation (Figure S6). Under such strong selection, a quarter of all individuals within each sex are expected to be excluded from reproduction (that is, to die during juvenile life) because of their maladaptive genotype at a single locus. Given that we observed dozens of genome regions showing even stronger intersex differentiation (Figures 1a, 2a, S4), it becomes clear from a purely theoretical perspective that SAS fails as a viable explanation for widespread intersex differentiation in our stickleback system; the total selection imposed by dozens of loci under such strong selection would be so intense that the population would go extinct rapidly.

Analytical implications

Our investigation has identified an alternative to sexually antagonistic selection as a cause for strong and widespread intersex allelic differentiation across autosomes: the copying of autosomal chromosome segments into a sex chromosome not represented in the reference genome assembly ('autosomal' here includes the pseudoautosomal region of the sex chromosome, as this regions also harbored SNPs exhibiting high intersex differentiation; Figure S4). Our work in no way challenges the notion that SAS could be widespread across the genome. However, the above (and previous; Kasimatis, Nelson, & Phillips, 2017) theoretical considerations indicate that intersex differentiation maintained by continuous sexually antagonistic viability selection within a population should be subtle in magnitude. The much stronger intersex differentiation arising artificially from incomplete genome assembly is thus likely to preclude the reliable investigation of the genomic consequences of SAS based exclusively on intersex differentiation data in this and analogous study systems. Although one could consider filtering genome regions based on the difference in MAF and/or imbalance in

read depth between the sexes, we doubt that this would completely eliminate spurious autosomal signals of SAS. The reason is that sex-related genetic differentiation and differences in MAF and read depth due to the mechanism described in Figure 5 may well remain subtle if an autosomal segment harboring a distinct genetic variant was copied relatively recently to the Y chromosome and still segregates at low frequency in the new chromosomal location. The availability of a complete genome assembly including *both* sex chromosomes, and the rigorous elimination of sequences aligning to any of them, may potentially allow detecting genome-wide signatures of SAS based on intersex differentiation data alone (Lucotte et al., 2016), although the reliability of such approaches awaits validation. We also note that if the transfer of autosomal sequences to the Y chromosome includes genes that retain expression in the new location (Mahajan & Bachtrog, 2017; Tsai et al., 2019), autosomal genes may appear to show concurrent intersex differences in both allele frequency and gene expression levels when ignoring copies on a missing sex chromosome.

In the vast majority of organisms used for genomic investigations, the Y (or W) chromosome sequence is not available, thus providing the opportunity for spurious intersex differentiation due to sex chromosome evolution. This has immediate implications to population genomics: in marker-based comparisons of populations, localized genome regions exhibiting high differentiation – often interpreted as hotspots harboring polymorphisms targeted by divergent selection between the populations – may emerge simply because the population samples differ in their proportion of females and males, and hence in the proportion of the two sex chromosomes (Benestan et al., 2017). To illustrate this point in our system, we drew 42 total nucleotides without replacement from the female and male nucleotide pool at all SNPs located within the chromosome window shown in Figure 2. Next, we combined 14 nucleotides from the female pool with 28 nucleotides from the male pool to obtain a first population sample, while the exactly opposite sexual representation was chosen for the second population sample. The outcome thus mimicked two random samples of 21 total diploid individuals from the same biological population, differing, beyond stochasticity in allele sampling, only in the sex ratio. We then calculated the magnitude of population differentiation across this chromosome window and observed, as expected, that the SNPs showing the highest population differentiation co-localized with the peaks in intersex differentiation (compare Figure 2d to 2a; Figure S3 shows this comparison based on F_{ST}). Ignoring imbalance in sex ratio may thus mislead the interpretation of patterns in population differentiation. This echoes an analogous caveat raised recently in a study of two species (American lobster and Arctic Char) in which sex-specific differentiation outliers were observed in genome scans comparing the sexes (Benestan et al., 2017). However, in that study, reference genomes for the focal species were not available. HIDRs were therefore

interpreted to reflect divergence between chromosome regions evolving sex-specifically, but the HIDRs could not be physically localized reliably. Our stickleback work extends these insights: even in an organism with a well-characterized sex determination system and an identified sex chromosome, HIDRs can occur on autosomes when one sex chromosome is missing (or incomplete) in the genome assembly and population samples differ in sex ratios. We also highlight the possibility that under these conditions, HIDRs may be influential enough to bias marker-based genomic analyses beyond simple differentiation, such as phylogenies or demographic reconstruction.

ACKNOWLEDGEMENT

We thank Elodie Burcklen and Christian Beisel for carrying out the sequencing at the Department of Biosystems Science and Engineering (D-BSEE, ETH Zürich), and the developers of Novocraft for sharing their aligner. Analysis of whole-genome data was performed at the Center for Scientific Computing at the University of Basel (sciCORE), and was aided by Francisco Pina-Martins. Katie Peichel and Astrid Böhne provided valuable suggestions for analysis. This study was supported by the Swiss National Science Foundation SNF (grants 31003A_165826 to DB and P300PA_174344 to MR), and by the University of Basel.

DATA AVAILABILITY

Raw sequence reads for the female and male pool are available from NCBI's sequence read archive under the BioSample accession numbers SAMN12777444 and SAMN12777445. Nucleotide counts across all genome-wide positions for the female and male pool, descriptive information on the HIDR SNPs, and the R code used for simulations of intersex differentiation are available on Dryad (doi: XXX).

AUTHOR CONTRIUBTIONS

M.B. performed wet lab work, carried out analyses, and wrote a first manuscript draft
T.G.L. performed wet lab work, wrote code for and performed cluster computation
M.R. stimulated the study and performed preliminary analyses

454 D.B. designed and supervised the study, wrote analytical code, analyzed and interpreted data,
455 and wrote the final manuscript, with feedback from M.R and T.G.L.
456

References

Aguirre WE, Akinpelu O (2010) Sexual dimorphism of head morphology in threespine stickleback (*Gasterosteus aculeatus*) *J. Fish Biol.* **77**, 802-821.

Arnqvist GRL (2005) *Sexual conflict* Princeton University, Princeton.

Benestan L, Moore J-S, Sutherland BJG*, et al.* (2017) Sex matters in massive parallel sequencing: evidence for biases in genetic parameter estimation and investigation of sex determination systems. *Mol. Ecol.* **26**, 6767-6783.

Berner D (2019) Allele frequency difference AFD - an intuitive alternative to FST for quantifying genetic population differentiation. *Genes* **10**, 308.

Berner D, Ammann M, Spencer E*, et al.* (2017) Sexual isolation promotes divergence between parapatric lake and stream stickleback. *J. Evol. Biol.* **30**, 401-411.

Berner D, Roesti M (2017) Genomics of adaptive divergence with chromosome-scale heterogeneity in crossover rate. *Mol. Ecol.* **26**, 6351-6369.

Berner D, Roesti M, Bilobram S*, et al.* (2019) *De novo* sequencing, assembly, and annotation of four threespine stickleback genomes based on microfluidic partitioned DNA libraries. *Genes* **10**, 426.

Berner D, Roesti M, Hendry AP, Salzburger W (2010) Constraints on speciation suggested by comparing lake-stream stickleback divergence across two continents. *Mol. Ecol.* **19**, 4963-4978.

Berner D, Thibert-Plante X (2015) How mechanisms of habitat preference evolve and promote divergence with gene flow. *J. Evol. Biol.* **28**, 1641-1655.

Bolnick DI, Lau OL (2008) Predictable patterns of disruptive selection in stickleback in postglacial lakes. *Am. Nat.* **172**, 1-11.

Chalopin D, Volff J-N, Galiana D, Anderson JL, Schartl M (2015) Transposable elements and early evolution of sex chromosomes in fish. *Chromosome Res.* **23**, 545-560.

Cheng CD, Kirkpatrick M (2016) Sex-specific selection and sex-biased gene expression in humans and flies. *PLoS Genet.* **12**.

Connallon T, Clark AG (2014) Balancing selection in species with separate sexes: insights from Fisher's geometric model. *Genetics* **197**, 991-1006.

Cox R, Calsbeek R (2009) Sexually antagonistic selection, sexual dimorphism, and the resolution of intralocus sexual conflict. *Am. Nat.* **173**, 176-187.

Darwin C (1871) *The descent of man, and selection in relation to sex* John Murray, London.

Dou J, Zhao X, Fu X*, et al.* (2012) Reference-free SNP calling: improved accuracy by preventing incorrect calls from repetitive genomic regions. *Biol. Direct* **7**, 17.

Dutoit L, Mugal CF, Bolivar P*, et al.* (2018) Sex-biased gene expression, sexual antagonism and levels of genetic diversity in the collared flycatcher (*Ficedula albicollis*) genome. *Mol. Ecol.* **27**, 3572-3581.

Ferretti L, Ramos-Onsins SE, Pérez-Enciso M (2013) Population genomics from pool sequencing. *Mol. Ecol.* **22**, 5561-5576.

Gautier M, Foucaud J, Gharbi K*, et al.* (2013) Estimation of population allele frequencies from next-generation sequencing data: pool-versus individual-based genotyping. *Mol. Ecol.* **22**, 3766-3779.

Glazer AM, Killingbeck EE, Mitros T, Rokhsar DS, Miller CT (2015) Genome assembly improvement and mapping convergently evolved skeletal traits in sticklebacks with genotyping-by-sequencing. *G3-Genes Genomes Genetics* **5**, 1463-1472.

Griffin RM, Dean R, Grace JL, Ryden P, Friberg U (2013) The shared genome is a pervasive constraint on the evolution of sex-biased gene expression. *Mol. Biol. Evol.* **30**, 2168-2176.

Hobza R, Cegan R, Jesionek W*, et al.* (2017) Impact of repetitive elements on the Y chromosome formation in plants. *Genes* **8**, 302.

Innocenti P, Morrow EH (2010) The sexually antagonistic genes of *Drosophila melanogaster*. *PLoS Biol.* **8**, e1000335.

Jones FC, Grabherr MG, Chan YF*, et al.* (2012) The genomic basis of adaptive evolution in threespine sticklebacks. *Nature* **484**, 55-61.

Kasimatis KR, Nelson TC, Phillipps PC (2017) Genomic signatures of sexual conflict. *J. Hered.* **108**, 780-790.

513 Kitano J, Mori S, Peichel CL (2007) Sexual dimorphism in the external morphology of the
514 threespine stickleback (*Gasterosteus aculeatus*). *Copeia* **2007**, 336-349.

515 Koerich LB, Wang XY, Clark AG, Carvalho AB (2008) Low conservation of gene content in the
516 *Drosophila* Y chromosome. *Nature* **456**, 949-951.

517 Kristjansson BK, Skulason S, Noakes DLG (2002) Morphological segregation of Icelandic
518 threespine stickleback (*Gasterosteus aculeatus* L). *Biol. J. Linn. Soc* **76**, 247-257.

519 Lucotte EA, Laurent R, Heyer E, Ségurel L, Toupance B (2016) Detection of allelic frequency
520 differences between the sexes in humans: a signature of sexually antagonistic selection.
521 *Genome Biol. Evol.* **8**, 1489-1500.

522 Mahajan S, Bachtrog D (2017) Convergent evolution of Y chromosome gene content in flies.
523 *Nat. Commun.* **8**, 785.

524 Mank JE (2017) The transcriptional architecture of phenotypic dimorphism. *Nat. Ecol. Evol.* **1**.

525 Manly BFJ (2006) *Randomization, bootstrap and Monte Carlo methods in biology*, 3rd edn.
526 Chapman & Hall, Boca Raton.

527 McKinney GJ, Waples RK, Seeb LW, Seeb JE (2017) Paralogs are revealed by proportion of
528 heterozygotes and deviations in read ratios in genotyping-by-sequencing data from natural
529 populations. *Mol. Ecol. Res.* **17**, 656-669.

530 Morgan M, Pages H, Obenchain V, Hayden N (2018) Rsamtools: binary alignment (BAM),
531 FASTA, variant call (BCF), and tabix file import. R package version 1.3.0
532 (http://bioconductor.org/packages/release/bioc/html/Rsamtools.html).

533 Moser D, Roesti M, Berner D (2012) Repeated lake-stream divergence in stickleback life history
534 within a Central European lake basin. *PLoS ONE* **7**, e50620.

535 Östlund-Nilsson S, Mayer I, Huntingford FA (2007) Biology of the three-spined stickleback. CRC,
536 Boca Raton.

537 Peichel CL, Ross JA, Matson CK*, et al.* (2004) The master sex-determination locus in threespine
538 sticklebacks is on a nascent Y chromosome. *Curr. Biol.* **14**, 1416-1424.

539 Poissant J, Wilson AJ, Coltman DW (2010) Sex-specific genetic variance and the evolution of
540 sexual dimorphism: a systematic review of cross-sex genetic correlations. *Evolution* **64**, 97-
541 107.

R Core Team (2017). R: A language and environment for statistical computing. R Foundation for Statistical Computing, Vienna, Austria.

URL https://www.R-project.org/.

Reimchen TE, Nosil P (2001) Ecological causes of sex-biased parasitism in threespine stickleback. *Biol. J. Linn. Soc.* **73**, 51-63.

Reimchen TE, Nosil P (2004) Variable predation regimes predict the evolution of sexual dimorphism in a population of threespine stickleback. *Evolution* **58**, 1274-1281.

Rice WR, Chippindale AK (2001) Intersexual ontogenetic conflict. *J. Evol. Biol.* **14**, 685-693.

Roesti M, Kueng B, Moser D, Berner D (2015) The genomics of ecological vicariance in threespine stickleback fish. *Nat. Commun.* **6**, 8767.

Roesti M, Moser D, Berner D (2013) Recombination in the threespine stickleback genome - patterns and consequences. *Mol. Ecol.* **22**, 3014-3027.

Roesti M, Salzburger W, Berner D (2012) Uninformative polymorphisms bias genome scans for signatures of selection. *BMC Evol. Biol.* **12**, 94.

Selander RK (1966) Sexual dimorphism and differential niche utilization in birds. *Condor* **68**, 113-151.

Shine R (1989) Ecological causes for the evolution of sexual dimorphism - a review of the evidence. *Quart. Rev. Biol.* **64**, 419-461.

Slatkin M (1984) Ecological causes of sexual dimorphism. *Evolution* **38**, 622-630.

Spoljaric MA, Reimchen TE (2008) Habitat-dependent reduction of sexual dimorphism in geometric body shape of Haida Gwaii threespine stickleback. *Biol. J. Linn. Soc.* **95**, 505-516.

Stewart AD, Pischedda A, Rice WR (2010) Resolving intralocus sexual conflict: genetic mechanisms and time frame. *J. Hered.* **101**, S94-S99.

Tsai KL, Evans JM, Noorai RE, Starr-Moss AN, Clark LA (2019) Novel Y chromosome retrocopies in canids revealed through a genome-wide association study for sex. *Genes* **10**, 320.

569 Williams TM, Carroll SB (2009) Genetic and molecular insights into the development and
570 evolution of sexual dimorphism. *Nat. Rev. Genet.* **10**, 797-804.

571

572 **Figure 1.** (a) Distribution of the magnitude of genetic differentiation between female and male
573 stickleback, as quantified by the absolute allele frequency difference AFD, across 1.63 million
574 autosomal single-nucleotide polymorphisms. In (b), intersex differentiation is mapped along a
575 representative chromosome.
576
577

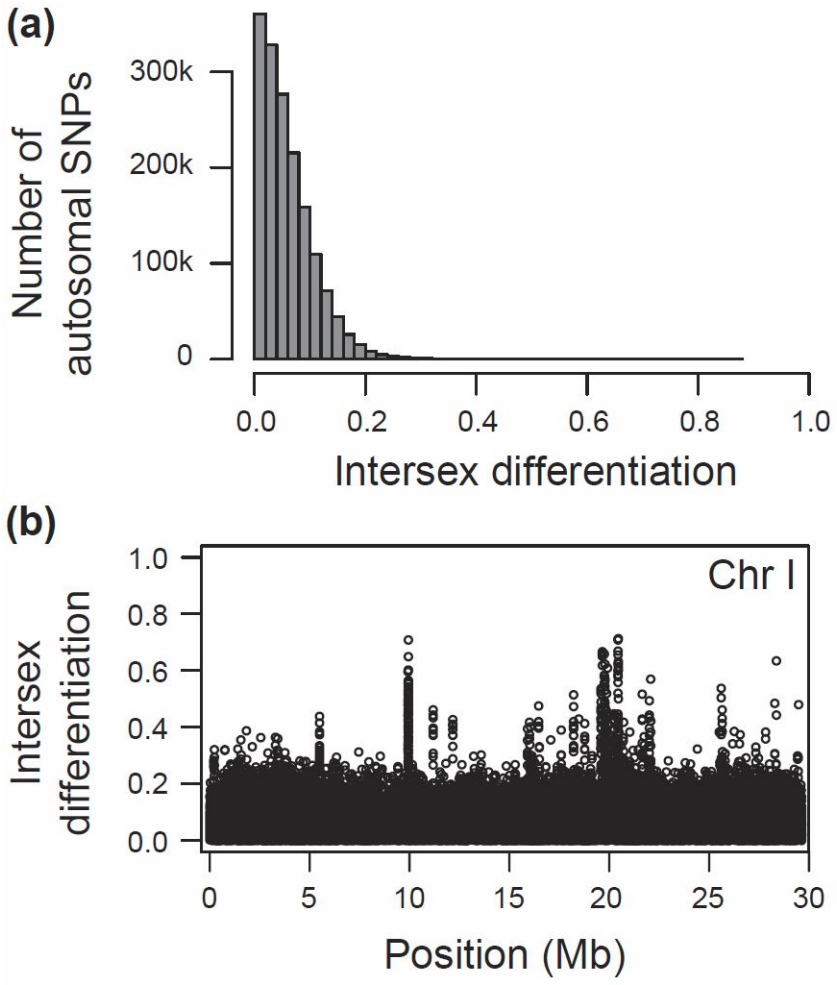

578
579
580
581
582

Figure 2. Characterization of a 100 kilobase segment on chromosome XI containing a representative region of high differentiation between female and male stickleback. (a) Genetic differentiation (AFD) between the sexes at single-nucleotide polymorphisms (SNPs) showing a pooled minor allele frequency (MAF) of at least 0.15. (b) Difference between the sexes in the MAF, considering all SNPs passing a pooled MAF threshold of 0.01. Positive values indicate that the two alleles at a SNP occur in more balanced proportion in males than in females. (c) Read depth in males standardized by the depth in females. High values indicate that male reads are relatively overrepresented in the sequencing output overlapping the corresponding genome positions. Note that because this statistic is calculated for every base position (not just the SNPs), a smoother (LOESS; moving average with a span of 0.002) was chosen for visualization to reduce complexity. (d) Genetic differentiation (AFD) between two population samples with symmetrical sex bias in opposite directions generated by re-sampling empirically observed female and male nucleotide data at each SNP.

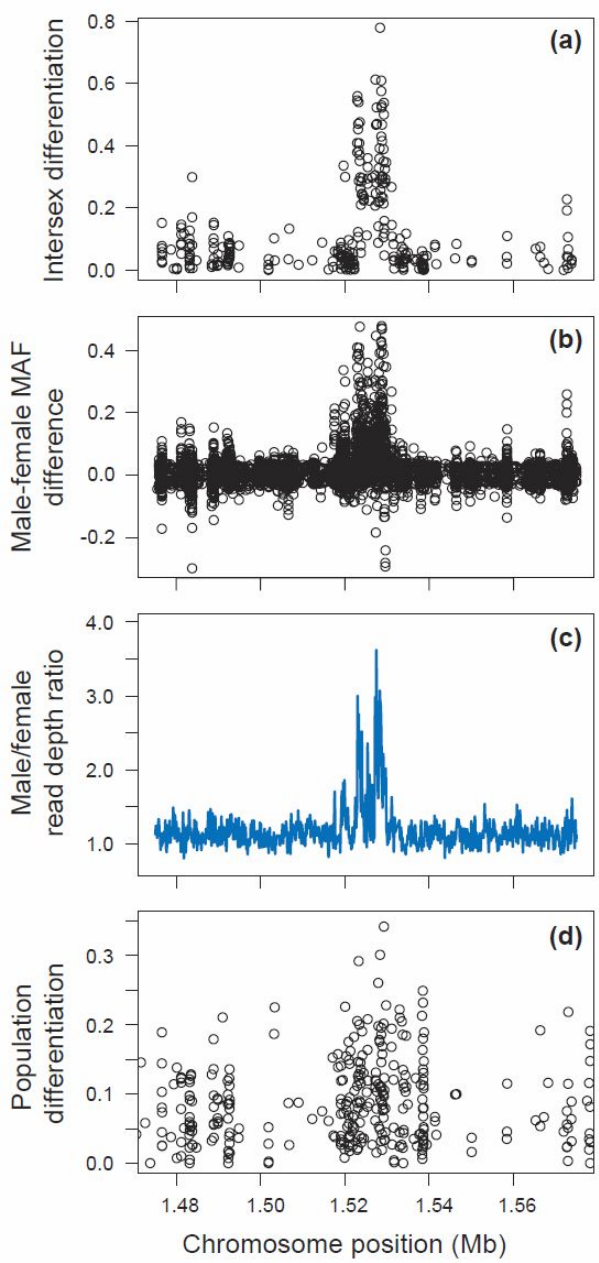

597 **Figure 3.** Frequency of the minor allele in females and males at 38 SNPs representing
598 independent regions of high intersex differentiation (HIDR SNPs), and at their associated control
599 SNPs.
600
601

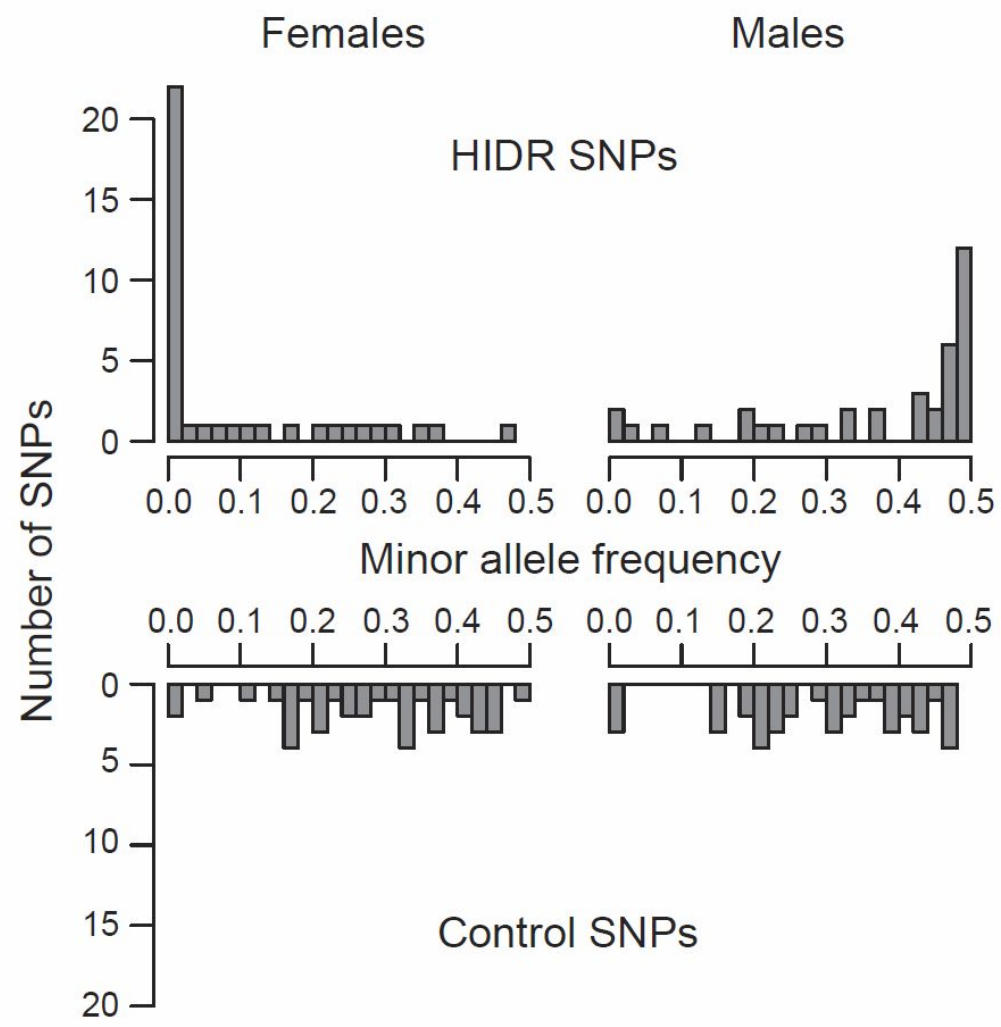

602

Figure 4. Ratio of the male by female read depth at the HIDR and control SNPs. Shown are the raw data points along with their median (black vertical line) and the 95% bootstrap confidence (gray box) for the median within each SNP class. The gray vertical line indicates balanced read depth between the sexes (note that all observed read depth ratios are slightly biased upward due to deeper sequencing of the male pool). To increase visual resolution, a single HIDR SNP showing an extreme read depth ratio (4.89) was omitted.

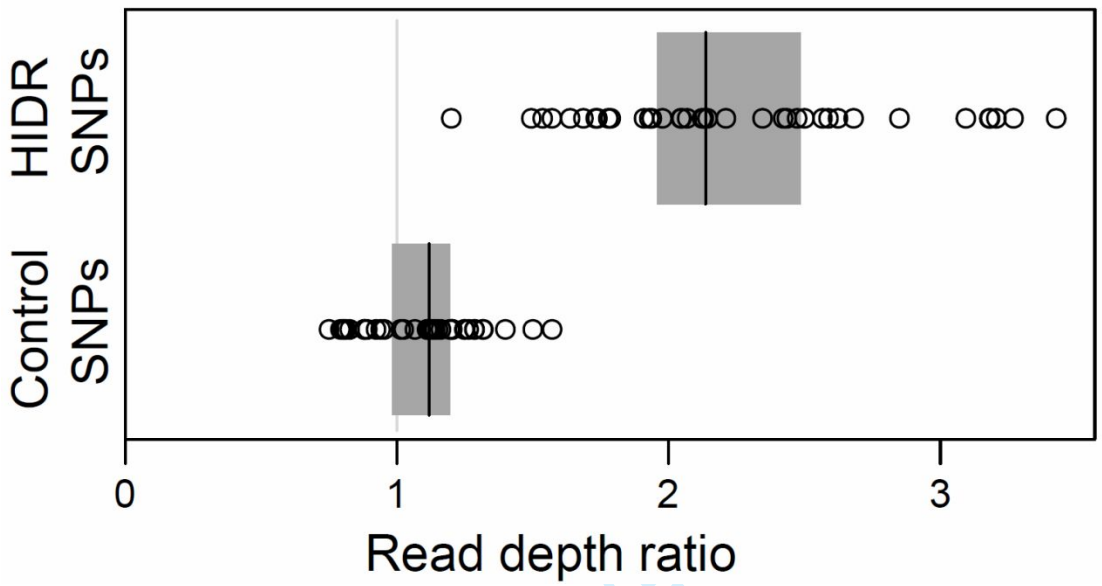

Figure 5. Schematic of the model explaining the emergence of HIDRs when a sex chromosome is missing in the genome assembly. First, an autosomal DNA segment (light blue) is copied into the Y chromosome. Mutation then generates polymorphisms distinguishing the original autosomal segment from its copy on the Y (indicated by the distinct blue shades). The Y-copy may then become multiplied further on that chromosome. As a consequence, DNA sequences from both the autosomal segment and its copies on the Y align to the same autosomal location when the reference genome lacks the Y chromosome. The analytical outcome is that males tend to display a more variable genotype (hence a higher MAF) than the females, and hence that the sexes show substantial allele frequency differentiation, at the distinctive polymorphisms. Moreover, male read depth is elevated across the entire focal DNA segment relative to females.

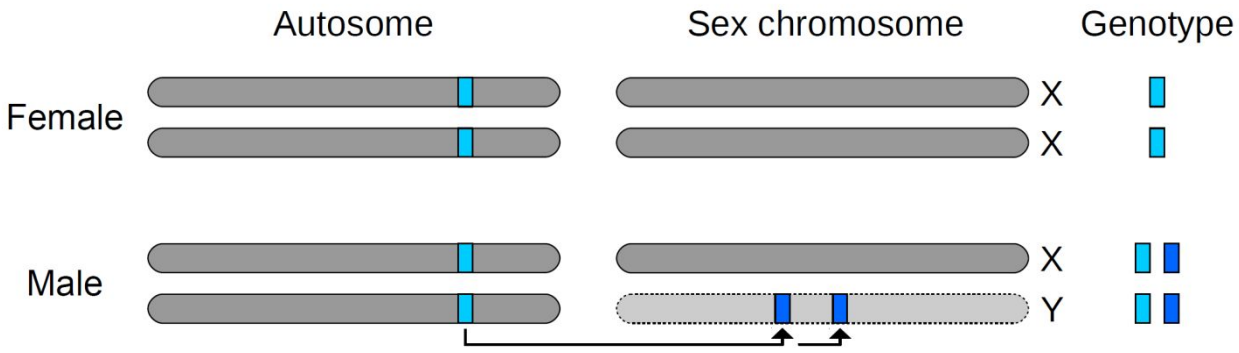

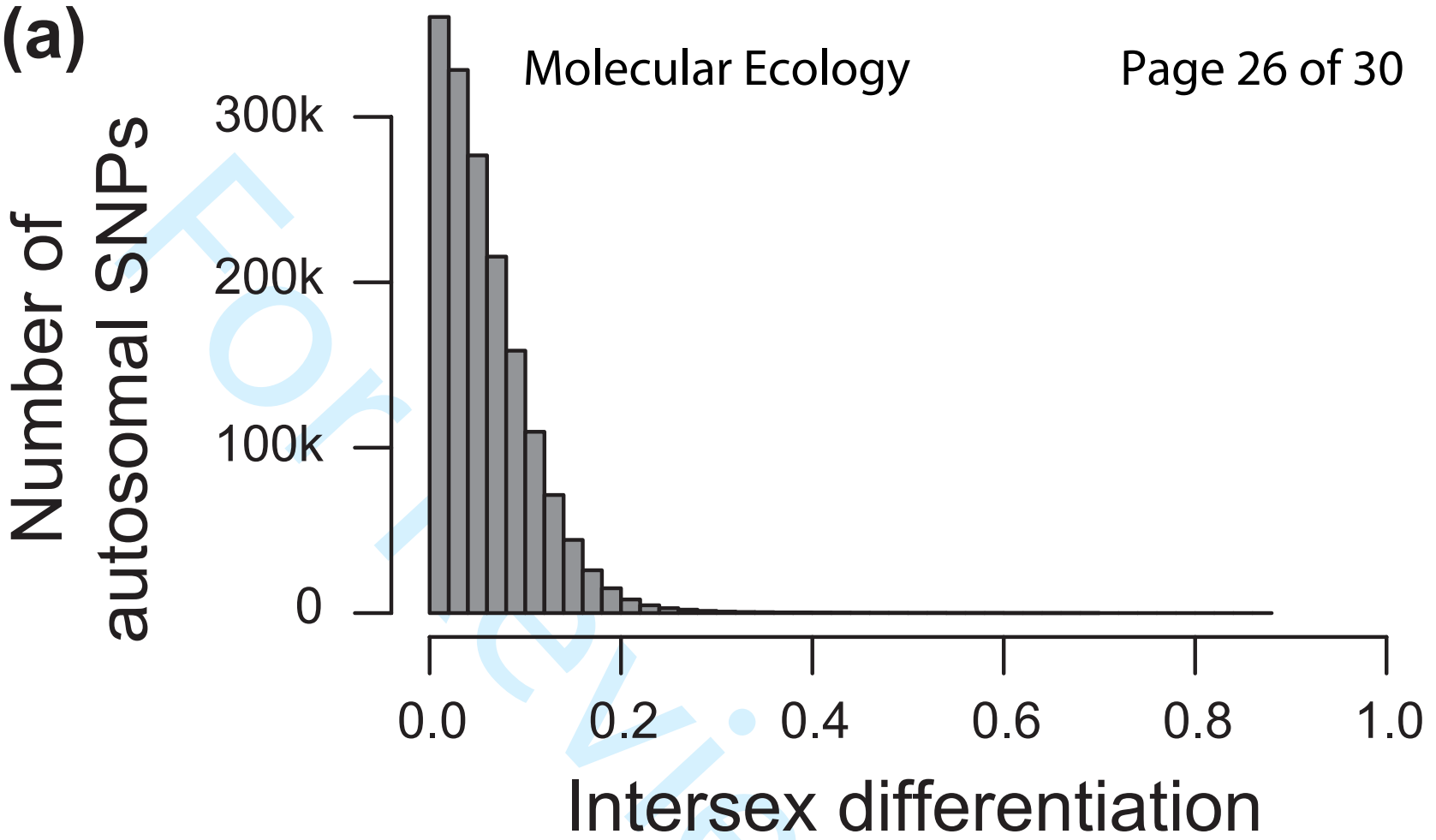

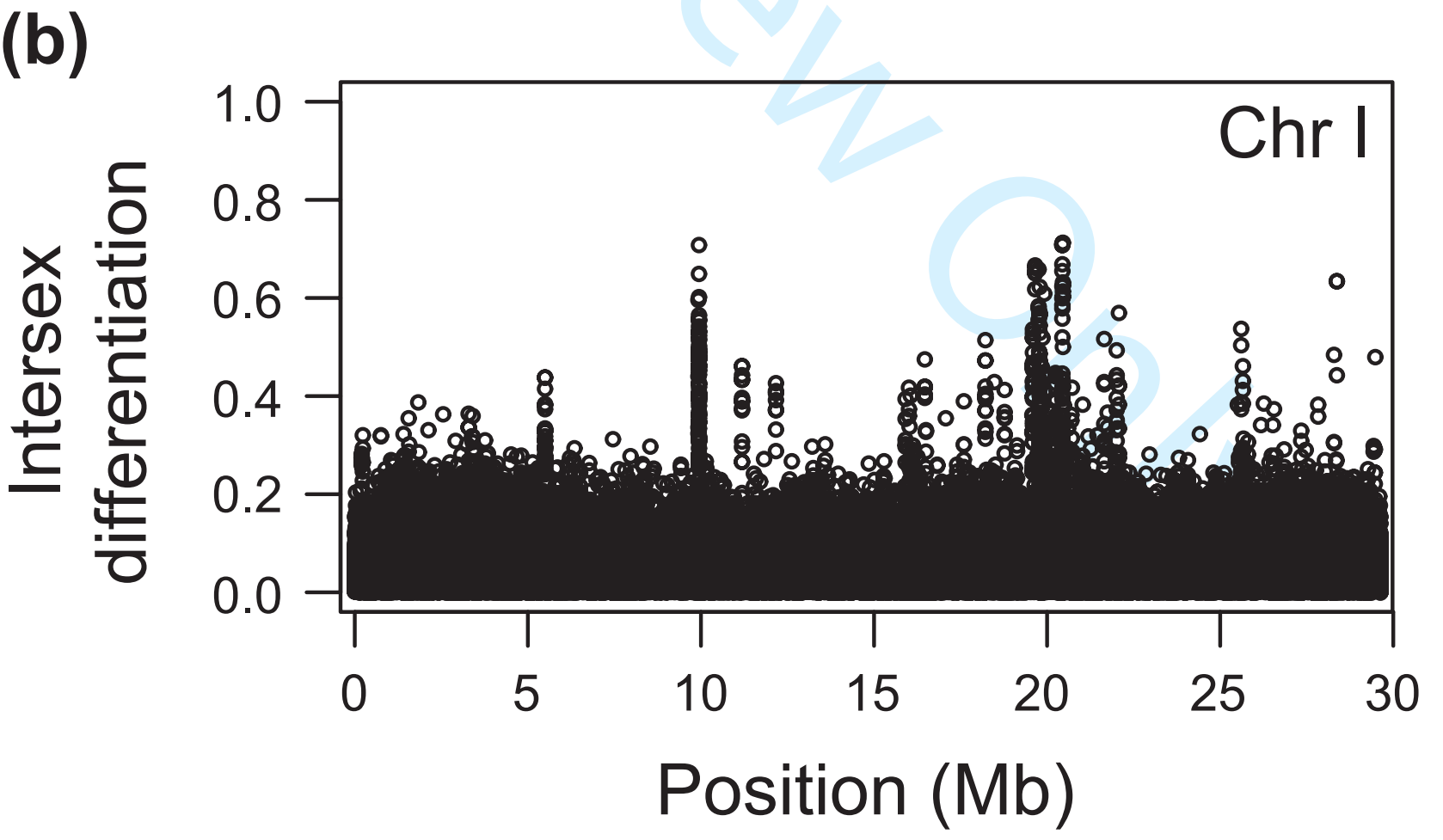

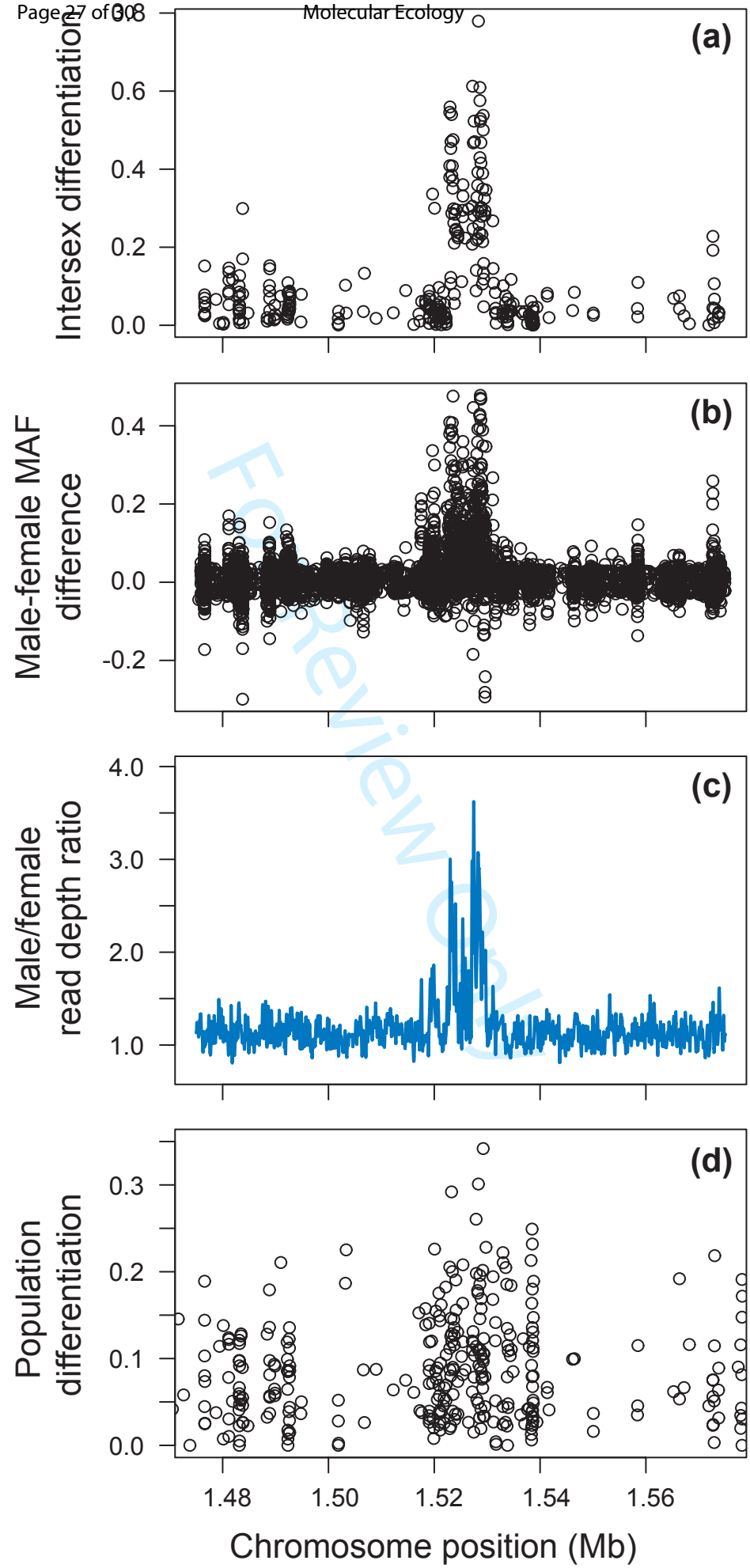

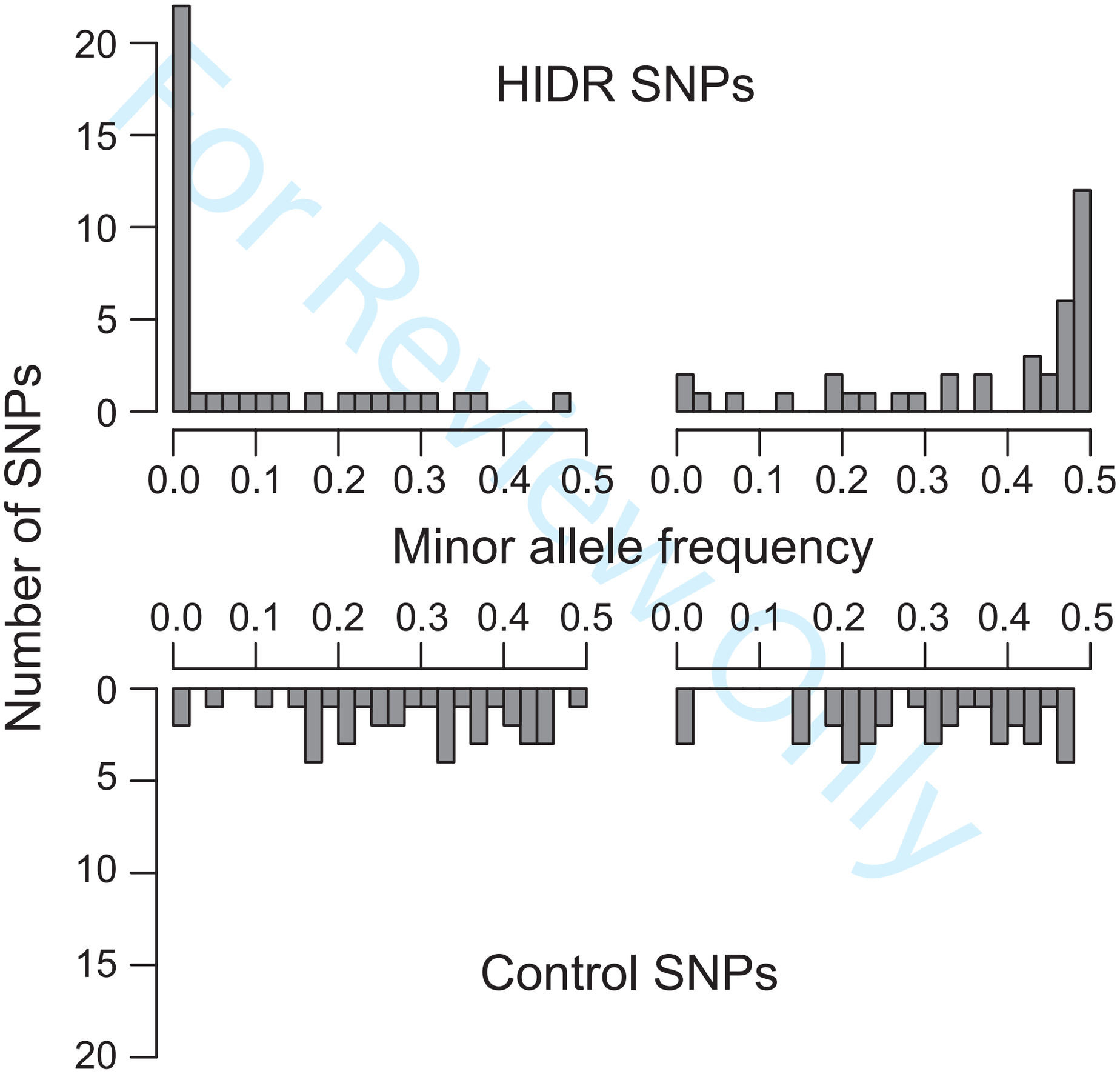

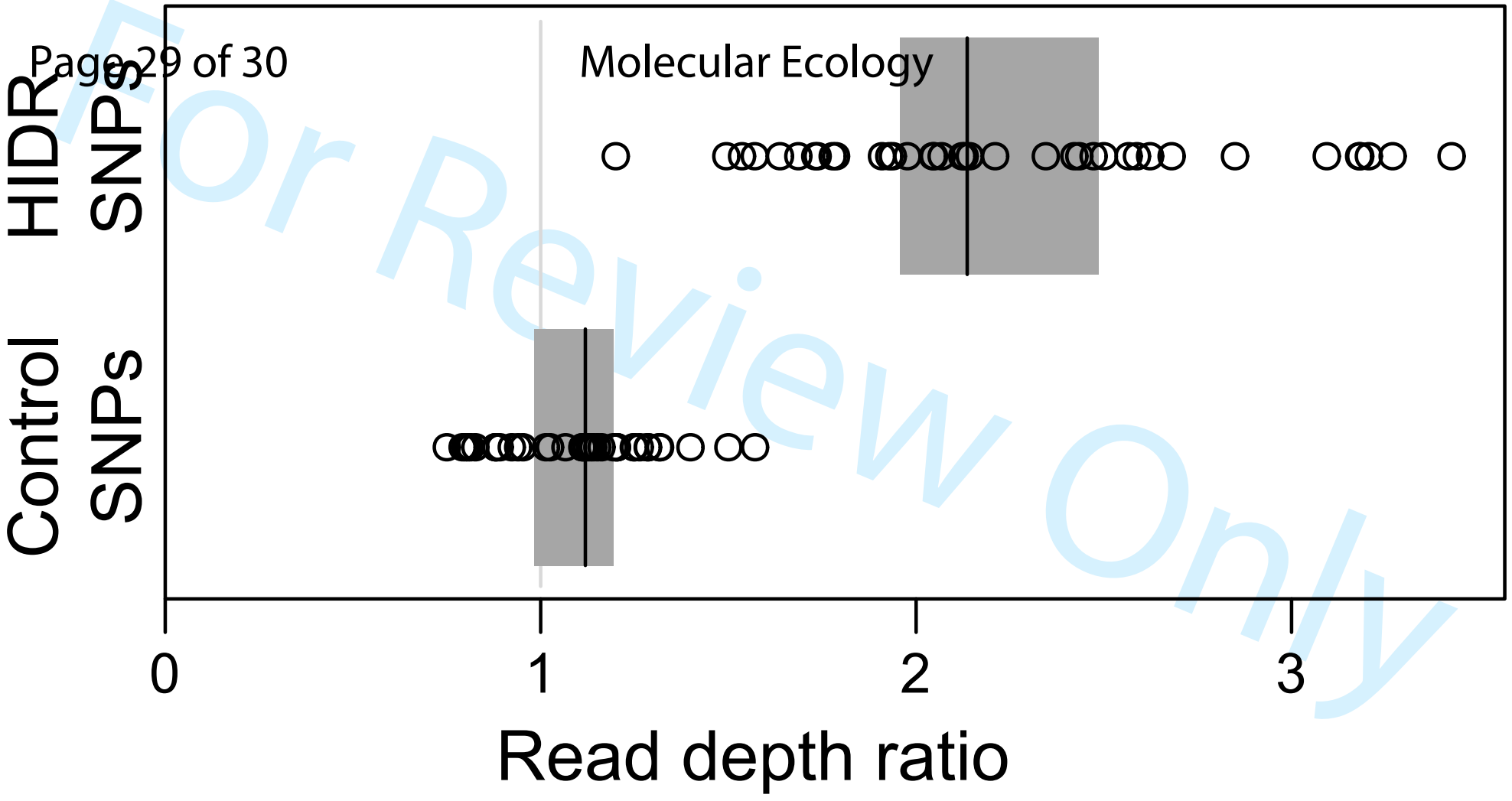

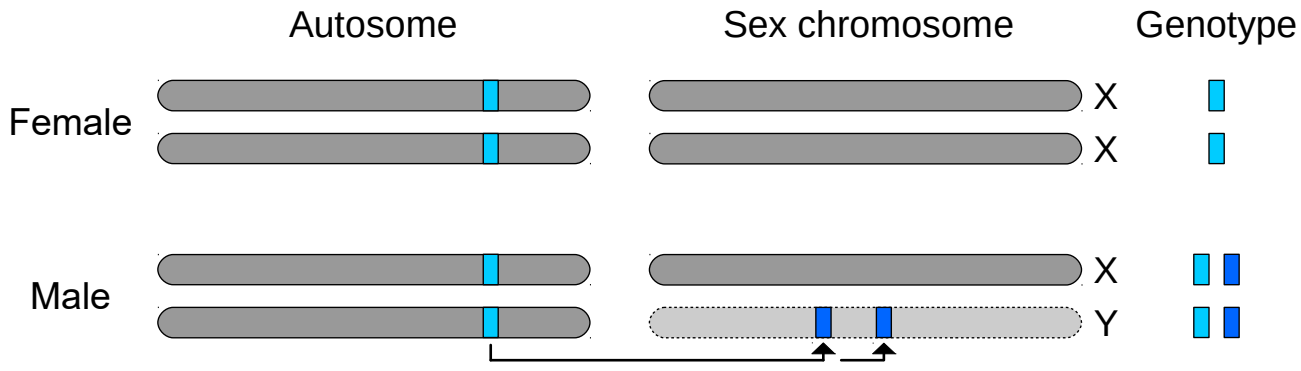
Autosome
Sex chromosome
Genotype
Female
X
X
Male
X
Y